A morphological analysis for searches of possible extended γ-ray sources associated with dark matter annihilation

D. Prokhorov, S. de Jong

Monthly Notices of the ROYAL ASTRONOMICAL SOCIETY
MNRAS **441,** 2200–2207 (2014) doi:10.1093/mnras/stu702

A morphological analysis for searches of possible extended γ-ray sources associated with dark matter annihilation

D. A. Prokhorov[1]★ and S. de Jong[2]

[1]*Max-Planck-Institut für Astrophysik, Karl-Schwarzschild-Strasse 1, D-85741 Garching, Germany*
[2]*François Arago Centre, APC, Université Paris Diderot, CNRS/IN2P3, CEA/Irfu, Observatoire de Paris, Sorbonne Paris Cité, 10 rue Alice Domon et Léonie Duquet, F-75205 Paris Cedex 13, France*

Accepted 2014 April 7. Received 2014 April 7; in original form 2014 January 22

ABSTRACT

We propose a morphological analysis for searches of extended γ-ray emission associated with dark matter annihilation. Our approach is based on the likelihood analysis including the spatial templates produced by taking into account the residual count maps in the energy band where the dark matter annihilation spectrum has a prominent spectral feature. The approach is tested on the example of the possible dark matter annihilation signal from the Virgo cluster of galaxies.

Key words: methods: data analysis – gamma-rays: diffuse background – gamma-rays: galaxies: clusters.

1 INTRODUCTION

Model selection is an important part of any statistical analysis (Burnham & Anderson 2002). One needs to make assumptions about the completeness of a model taking into account relevant physical processes. Residual count maps, obtained from the subtraction of the modelled count map (obtained as the result of a likelihood analysis) from the observational data, can contain spatial or spectral structures. These structures are more likely due to imperfections of the selected model rather than the evidence for a new physical process. In this paper, we analyse the data taken by the *Fermi* Large Area Telescope (LAT) from the region including the Virgo cluster of galaxies and propose a method to test the presence of a possible extended γ-ray source.

A number of astrophysical source classes including supernova remnants, pulsar wind nebulae, molecular clouds, normal galaxies, and clusters of galaxies are expected to be spatially extended and resolvable by the *Fermi*-LAT. Normal galaxies and galaxy clusters contain large amounts of dark matter (DM; for a review, see Trimble 1987). The analysis of spatially extended objects is more complex compared with that of point-like objects, because the extension of an object adds an additional degree of freedom to the model. The LAT has firmly detected 12 extended γ-ray sources (including three normal galaxies) during the first 2 yr of the *Fermi* mission (for a catalogue, see Nolan et al. 2012). Lande et al. (2012) have reported nine additional extended objects, detected using 2 yr of *Fermi*-LAT data. Galaxy clusters are promising candidates to γ-ray emitting sources which can potentially be discovered by *Fermi*-LAT (e.g. see Miniati 2003; Pinzke, Pfrommer & Bergström 2011).

★E-mail: phdmitry@mpa-garching.mpg.de

To search for a spatially extended object on the maps of *Fermi*-LAT, one needs to assume its spatial morphology and spectrum. One of the methods to make such assumptions is to adopt a spatial template associated with emission observed in a different energy band, e.g. at radio or X-ray frequencies. Due to different radiative processes contributing at different frequencies, this method gives no guarantee that the spatial morphologies are similar in different energy bands. Another method is to choose the shape of the photon spectrum, e.g. a power law, but the photon spectrum of a candidate source is a priori unknown. The likelihood ratio test allows us to compare candidate models, and as such to determine which candidate model gives the best description of the data. The set of models can, however, never be totally complete and the likelihood ratio test can be applied only for a comparison of nested candidate models (one candidate model is a special case of the other).

Residual count maps can be used to produce spatial templates and to determine spectral shapes for new extended γ-ray source candidates. This technique can be successfully used if foreground and background emission are perfectly modelled. However, there are some uncertainties in the determination of foreground and background emission. In this paper, we will present, and apply, a method to test the presence of spatially extended objects. This method is based on the analysis of assumptions on the spectral and spatial properties of a potential extended source. These assumptions are adopted in a model where source candidates are present and their presence is consistent with observations at the high statistical significance. If the modification to the assumptions (e.g. of spatial symmetry) results in a strong decrease of the statistical significance of a candidate extended object then the model should be reconsidered.

Below we discuss how to search for the presence of extended γ-ray emission from the Virgo cluster that could potentially be

produced via the annihilation of DM particles. The presented method will allow us to study the presence of extended emission associated with the Virgo cluster and can be applied for a search for extended objects associated with high DM concentrations, such as those in the Galactic Centre and Andromeda galaxy, in the future.

2 APPARENT EXTENDED EMISSION FROM THE DM HALO IN VIRGO

Clusters of galaxies are the largest gravitationally bound structures in the Universe, with sizes of $\simeq$1–3 Mpc, containing hundreds of galaxies and a hot ($\simeq$1–10 keV) diffuse plasma which sets in equilibrium in the potential wells of the clusters (for a review, see Sarazin 1986). The presence of non-baryonic matter, known as DM, was inferred from its gravitational effects on visible matter. The DM component contributes $\simeq$80 per cent to the total mass of a galaxy cluster, $M_{\rm cluster} \simeq 10^{14}$–$10^{15}$ $M_{\odot}$. The nature of DM remains unknown. Weakly interacting massive particles (WIMPs) are hypothetical particles serving as one possible solution to the DM problem and are predicted by many new physics models beyond the standard model of particle physics (for a review, see Bertone, Hooper & Silk 2005). γ-rays from annihilation of WIMPs in galaxy clusters could potentially be detected by *Fermi*-LAT (for a review of the present status of astrophysical searches for particle DM, see Porter, Johnson & Graham 2011). The search for GeV emission from clusters of galaxies using data collected by the LAT from 2008 August to 2010 February has been reported by Ackermann et al. (2010b), who derived γ-ray flux upper limits from galaxy clusters. Recently, Ackermann et al. (2013) and Prokhorov & Churazov (2013) performed a joint likelihood analysis of about 50 galaxy clusters without the inclusion of the nearest galaxy clusters with virial radii exceeding 1° and found no signature which can be associated with a signal from DM annihilation. A search for the possible γ-ray signatures of DM annihilation from the nearest galaxy clusters is of interest (e.g. see Ackermann et al. 2010a; Ando & Nagai 2012; Gao et al. 2012; Huang, Vertongen & Weniger 2012).

The Virgo cluster is located about 16.5 Mpc away and is the nearest large galaxy cluster. Due to Virgo's proximity, this cluster is an excellent target for γ-ray observations as it can spatially be resolved by *Fermi*-LAT at GeV energies. Recently, a signal consistent with that expected from DM annihilation from the Virgo cluster has been discussed by Han et al. (2012a), who have analysed the first 3 yr of data from *Fermi*-LAT. The reported signal is at a significant level of 4.4σ for a model in which WIMPs, with mass $M \simeq 28$ GeV, annihilate via the $b\bar{b}$ channel. A large boost factor, $\sim 10^3$, is invoked by Han et al. (2012a) for the DM interpretation of the observational data. Phoenix simulations by Gao et al. (2012) suggest the large enhancement of a flux (a boost of $\simeq$1000) due to substructures in galaxy clusters. Note that the constraints on cross-section in the $b\bar{b}$ channel obtained by Han et al. (2012a) are by one order of magnitude tighter than those derived from a joint analysis of the Milky Ways dwarf galaxies (Ackermann et al. 2014) and, therefore, a boost factor of the order of $\simeq$100 is required for the DM interpretation of the observations of the Virgo cluster with *Fermi*-LAT. Recent works by Ludlow et al. (2013) and Sanchez-Conde & Prada (2013) show that the flattening of the concentration–mass relation towards low halo masses lead to lower boost factors, $\simeq$35, for galaxy clusters than those relied on power-law extrapolations of the concentration–mass relation.

As was shown by Han et al. (2012b) and Macías-Ramírez et al. (2012), the tentative evidence for a γ-ray excess from the Virgo cluster is mainly due to a population of γ-ray point sources with power-law spectra near the Virgo cluster that are not included in the LAT 2-yr point source (2FGL) catalogue (Nolan et al. 2012). The 2FGL catalogue contains γ-ray point sources which are significantly with a TS > 25 (test-statistics; Mattox et al. 1996) detected by the LAT in the first 24-months of the *Fermi* mission. The new γ-ray point sources are found to be above the standard detection significance threshold when more than 2 yr of LAT data are used. The inclusion of several new point sources, that are above the threshold of TS = 25 threshold for the 4 yr data, in the original model of Han et al. (2012a) decreases the significance of the possible DM signal from the $\simeq 5\sigma$ level to $\simeq 3\sigma$ level (Han et al. 2012b; Macías-Ramírez et al. 2012).

Note that the presence of the central galaxy of M87, also a γ-ray source (Abdo et al. 2009), in the Virgo cluster complicates the analysis of this region, since the subtraction of M87 from the data is necessary for studying the possible extended component associated with the DM halo of the Virgo cluster. The separation of these two γ-ray emission components can be performed by analysing the emission at energies of $\gtrsim$1 GeV, where the full-width half-maximum of the point spread function (PSF) is less than the expected angular size of the DM halo. Annihilation of WIMPs of $M \simeq 28$ GeV should produce a γ-ray signal resulting in an excess at energies of $\simeq$1–3 GeV over the total emission from point sources, diffuse galactic foreground, and isotropic background (this excess should be owing to the specific spectral shape of emission from DM annihilation occurred via the $b\bar{b}$ channel, see Section 4). The excess of γ-ray emission from the Virgo cluster at $\simeq$1–3 GeV energies over that expected from 2FGL sources, diffuse galactic foreground, and isotropic background was demonstrated by Han et al. (2012a, see the right-hand panel of their fig. 12). The presence of this excess in the spectrum leads to the idea that the analysis of residual count maps at energies of a few GeV can be useful for studying the morphology of extended emission from the Virgo cluster. In this paper, we will prove the importance of a morphological analysis for the study of extended γ-ray sources.

3 OBSERVATION AND DATA REDUCTION

Fermi was launched on 2008 June 11 into a nearly circular Earth orbit with an altitude of 565 km and inclination of 25.°6, and an orbital period of 96 min. The principal instrument on *Fermi* is the LAT (Atwood et al. 2009), a pair-production telescope with a large effective area ($\sim$8000 cm^2 at 1 GeV) and field of view (2.4 sr), sensitive to γ-rays between 20 MeV and >300 GeV. After the commissioning phase, the *Fermi*-LAT began routine science operations on 2008 August 4. The detector normally operates in sky-survey mode which provides a full-sky coverage every 3 h (i.e. two orbits).

For the data analysis, we use the FERMI SCIENCE TOOLS v9r27p1 package[1] and P7V6 instrument response functions. We use accumulated events obtained from 2008 August 4 to 2012 June 12. Events $\geq$100 MeV arriving within 20° of M87 (region of interest – ROI) and satisfying the SOURCE event class are selected. To reduce the contamination by the γ-ray emission coming from cosmic ray (CR) interactions in the Earth's upper atmosphere, our selection is refined by choosing events with zenith angles <100°. We remove events that occur during manoeuvres when the *Fermi*-LAT rocking angle was larger than 52°.

Our aim is to study the morphologies of spatial structures on the residual count map of the Virgo cluster at energies of a few GeV.

[1] http://fermi.gsfc.nasa.gov/ssc/data/analysis/

Table 1. The list of the 16 strong sources in the ROI.

2FGLJ1158.8+0939	2FGLJ1204.2+1144
2FGLJ1209.7+1807	2FGLJ1214.6+1309
2FGLJ1214.8+1653	2FGLJ1222.4+0413
2FGLJ1224.9+2122	2FGLJ1229.1+0202
2FGLJ1230.8+1224	2FGLJ1231.6+1417
2FGLJ1239.5+0443	2FGLJ1239.5+0728
2FGLJ1251.2+1045	2FGLJ1256.1−0547
2FGLJ1301.5+0835	2FGLJ1305.0+1152

The residual count map is produced by subtracting the modelled count map, which is based on the result of a likelihood analysis, from the observational data. To demonstrate the approach for studying extended objects, we include the 2FGL point sources located within the ROI and the diffuse foreground and background in the model. The spectral shapes of the point sources are taken from the 2FGL catalogue (Nolan et al. 2012), while the normalizations and spectral parameters of sixteen strong point sources (including M87) are derived from the likelihood analysis (the list of the 16 strong sources are shown in Table 1). The normalizations of fainter point sources are held fixed at the 2FGL catalogue values. The Galactic diffuse foreground and isotropic diffuse background[2] are included in the model by the templates, gal_2yearp7v6_v0.fits and iso_p7v6source.txt, respectively. The normalizations of the galactic and isotropic components are allowed to vary during the fitting. Note that our model is more detailed than that of Han et al. (2012a), because the parameters of only three 2FGL point sources (within the Virgo's virial radius of 4.°6) have been allowed to vary in their analysis. As shown in fig. 1 of Han et al. (2012a), the three point sources within the Virgo's virial radius are faint and, therefore, the residuals are dominated by the contribution from stronger γ-ray sources which are outside the virial radius. This is due to their spectral parameters not perfectly described by the values taken from the 2FGL catalogue, since the data from a longer *Fermi*-LAT observation are analysed.

Since the values of the spectral parameters of the 16 strong point sources are derived from the likelihood analysis in our study, the calculated residual count maps (see Section 4) are more suitable for the morphological analysis. We will discuss the population of γ-ray point sources near the Virgo cluster which are not included in the 2FGL catalogue in Section 5, where the results of our likelihood analysis will be presented.

4 LIKELIHOOD ANALYSIS AND RESIDUAL COUNT MAP BETWEEN 1 AND 3 GEV

We analyse the first 3.8 yr of *Fermi*-LAT observations using the binned maximum likelihood mode of the *gtlike* routine, which is part of the FERMI SCIENCE TOOLS[1]. The test-statistic TS was employed to evaluate the significance of the γ-ray fluxes coming from the sources. The TS value is defined as twice the difference between the log-likelihood function maximized by adjusting all the parameters of the model, with $\log L_{\rm max,1}$ and without the source $\log L_{\rm max,0}$, via $\mathrm{TS} = 2(\log L_{\rm max,1} - \log L_{\rm max,0})$.

The choice of the free and fixed parameters in the analysis is described in Section 3. The list of the 16 point sources with spectral parameters left free in the fit is shown in Table 1. We set the energy binning to 30 logarithmic bins between 100 MeV and 300 GeV.

From the resulting best fit, we construct the model counts map in the 1–3 GeV band using the *gtmodel* tool from the FERMI SCIENCE TOOLS. We choose this energy interval because it corresponds to photon energies at which the γ-ray emission from DM annihilation of WIMPs with $M \simeq 28$ GeV via the $\mathrm{b\bar{b}}$ channel should strongly contribute to the total signal (see, e.g. Baltz, Taylor & Wai 2007). Note that the photon spectrum, $\mathrm{d}N/\mathrm{d}E$, corresponding to annihilation of WIMPs with $M \simeq 25$ GeV via the $\mathrm{b\bar{b}}$ channel can be approximated as an exponentially cut-off power-law function with $\Gamma = 1.22$ and $E_{\rm cut} = 1.8$ GeV (see Ackermann et al. 2012a)

$$\frac{\mathrm{d}N}{\mathrm{d}E} = N_0 \left(\frac{E}{E_0}\right)^{-\Gamma} \exp\left(\frac{-E}{E_{\rm cut}}\right), \quad (1)$$

where N_0 and E_0 are the pre-factor and the scale factor. The value of the exponential cut-off, $E_{\rm cut} = 1.8$ GeV, lies in the energy interval of (1 GeV, 3 GeV) and the spectral index, $\Gamma = 1.22$, is very hard at energies below the exponential cut-off compared with a typical spectral index of 2FGL point sources. Therefore, the flux excess in the 1–3 GeV energy range can be interpreted as the exponential break in the exponentially cut-off power-law spectrum of an additional component produced by DM annihilation.

This additional component is consistent with possible annihilation emission of DM particles with $M \simeq 28$ GeV and was found by Han et al. (2012a) in their likelihood analysis where a specific spatial DM template was used, based on high-resolution cosmological simulations by Gao et al. (2012), assuming DM annihilation spectra, and including only point sources from the 2FGL catalogue in the original model. Therefore, we suppose that this additional DM component can potentially also be revealed on the residual count map at 1–3 GeV by studying morphology of residuals.

To justify the use of the 1–3 GeV energy band for studying the morphology of the possible component associated with DM annihilation, we model the expected DM annihilation signal with the spectrum from equation (1), Galactic foreground, and isotropic background by using the *gtmodel* routine from the FERMI SCIENCE TOOLS. Modelling is performed for various energy bands with the minimum and maximum energy bounds logarithmically spaced between 500 MeV and 300 GeV. We use the average values of Galactic foreground flux within a region of 4×4 deg^2 and an extended DM annihilation signal uniformly filling the modelled region. The lowest energy bound is selected by taking the angular resolution of *Fermi*-LAT into account. The modelled ratio of the expected DM annihilation signal to the sum of Galactic foreground and isotropic background is shown in Fig. 1. The values of the modelled ratio in this figure are normalized to the highest value. Fig. 1 shows that the 1–3 GeV energy band is suitable for an analysis of the possible DM contribution to the total signal, since the values of (DATA-MODEL)/MODEL should be high in this energy band if a DM annihilation component with the given spectrum is present in the *Fermi*-LAT data. Note that ≈40 per cent of all photons with energies between 500 MeV and 300 GeV produced by DM annihilation lie in the 1–3 GeV energy band. The 68 per cent containment angle at energies higher 1 GeV is smaller than 1° and *Fermi*-LAT therefore allows us to perform an analysis of γ-ray emission from nearby clusters of galaxies based on spatial templates derived from the residual map in the 1–3 GeV band. The likelihood analyses in Section 5 will be performed by using 30 logarithmic bins between 100 MeV and 300 GeV and by using spatial templates based on the 1–3 GeV residual map.

[2] http://fermi.gsfc.nasa.gov/ssc/data/access/lat/BackgroundModels.html

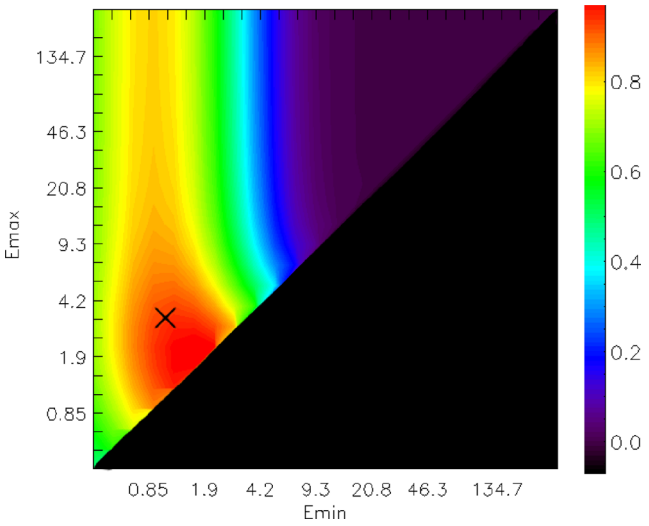

Figure 1. Normalized ratio of the expected DM annihilation signal to the sum of galactic foreground and isotropic background obtained by means of modelling. The value for the energy band of 1–3 GeV is shown with a cross.

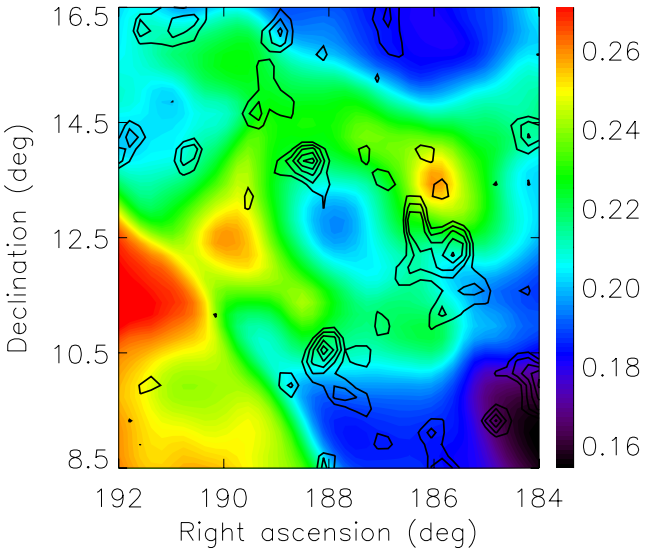

Figure 2. The relative residual count map for the energy range 1–3 GeV is shown by contour lines. This map was smoothed with a 2D Gaussian kernel of $\sigma = 0.^{\circ}4$. The contour levels correspond to values of 0.4, 0.6, 0.8, 1.0, and 1.2.

Fig. 2 shows the relative residual count map, (DATA-MODEL)/MODEL, of size $8^{\circ} \times 8^{\circ}$ (corresponding to 2.3 Mpc × 2.3 Mpc) with a pixel size of $0.^{\circ}1$ for the energy range 1–3 GeV by contour lines. This map is derived from the observed LAT count map by subtracting the model obtained from the likelihood analysis and is centred on the position of M87. The residual map was smoothed with a 2D Gaussian kernel of $\sigma = 0.^{\circ}4$. The contour levels correspond to values of 0.4, 0.6, 0.8, 1.0, and 1.2. The relative residual count map reveals three prominent structures near the Virgo cluster that have approximate coordinates $\simeq(188^{\circ}, 13.^{\circ}5)$, $\simeq(188^{\circ}, 10.^{\circ}5)$, and $\simeq(186^{\circ}, 12^{\circ})$. We also show the Galactic diffuse foreground model in the energy band of 1–3 GeV in Fig. 2 by colour.

The Galactic diffuse model (for a review, see Ackermann et al. 2012b) is taken from the spatial and spectral template, gal_2yearp7v6_v0.fits, provided by the *Fermi*-LAT collaboration.[3] This model for the Galactic diffuse emission was developed using spectral line surveys of H I and CO (as a tracer of H2) to derive the distribution of interstellar gas in Galactocentric rings. Infrared tracers of dust column density were used to correct column densities in directions where the optical depth of H I was either over- or underestimated. The model of the diffuse γ-ray emission was constructed by fitting the γ-ray emissivities of the rings in several energy bands to the LAT observations after removal of the point sources. In the southeastern quadrant of this map, the North Polar spur (the rim of a hot galactic super bubble) is contributing to the Galactic diffuse foreground emission model.

In the next section, we attempt to understand the origin of these three prominent structures on the 1–3 GeV residual count map and to discuss whether or not their origin can be caused by DM annihilation emission from the DM halo of the Virgo cluster. The aim of the following study is to demonstrate that the residuals at the exponential break energy of the assumed additional spectral component can be used for producing templates and that it is useful to include the spatial templates in the analysis in order to interpret the observations by means of a likelihood analysis.

5 LIKELIHOOD ANALYSIS AND MORPHOLOGY OF RESIDUALS

In this section, we make various spatial templates for the additional γ-ray component coming from the region of the Virgo cluster. We take the morphology of the residual count map at energies of 1–3 GeV into account and compare the models associated with the spatial templates using the likelihood ratio test for goodness of fit.

The dominant foreground γ-rays are produced by the neutral pion decay originating from interactions of CR protons with the interstellar medium (ISM). The γ-ray intensity from neutral pion decay is proportional to the integral along the line of sight of the product of the ISM density and the CR proton density. The resulting γ-ray distribution produced via neutral pion decay should be morphologically correlated with other maps of spatial tracers of the ISM, such as spectral lines of H I and CO, and dust continuum. Study of ISM tracers provides the information on the small-scale properties of the galactic diffuse emission.

Fig. 2 shows that the galactic diffuse emission is inhomogeneous in the region of the Virgo cluster and that the Galactic diffuse emission map of this region contains the spatial structure. This structure has the shape of a doughnut and its centre coincides with the position of M87. The three prominent structures on the residual count map at 1–3 GeV lie approximately on this γ-ray 'doughnut' structure (see Fig. 2). To clarify the origin of this structure on the Galactic diffuse emission map, we use the H I gas map obtained by the Leiden/Argentine/Bonn Survey of Galactic H I (Kalberla et al. 2005). The H I map contains a similar doughnut-shaped structure and that the positions of the H I gas structure and of the diffuse emission are spatially coincident. Further evidence for the gas 'doughnut' in the direction of the Virgo cluster comes from far-infrared observations. The *Herschel* Virgo Cluster Survey observed four 4 × 4 square degree regions towards the Virgo cluster (Davies et al. 2010; Auld et al. 2013). At a wavelength of 250 μm, the Galactic dust cirrus is seen in the 4 × 4 square degree map centred on M87 and is doughnut shaped (see the left-bottom panel of fig. 1 in Auld et al.

[3] http://fermi.gsfc.nasa.gov/ssc/data/access/lat/Model_details/Pass7_galactic.html

2013). The observations of both the H I and dust emission show a prominent doughnut-shaped structure towards the Virgo cluster.

Therefore, we conclude that the presence of the doughnut-shaped structure on the Galactic diffuse emission map is owing to the particular shape of the ISM gas spatial distribution in this region. Note that the residuals in the 1–3 GeV energy band for this $8^\circ \times 8^\circ$ region are highest on the gas structure and, therefore, the *Fermi*-LAT observations of this region are not described properly by the galactic diffuse template and 2FGL point sources.

5.1 Spatial templates

We create the first spatial template, dubbed *doughnut*, taking into account the approximate spatial coincidence of the locations of the foreground emission doughnut-shaped structure and of the high residuals at 1–3 GeV. This template is shown on the upper-left panel in Fig. 3. The radii of the inner and outer circular boundaries of the *doughnut* are $R_{\rm inner} = 1^\circ$ and $R_{\rm outer} = 2\overset{\circ}{.}2$, respectively, and were chosen according to the morphology of the structure on the Galactic diffuse emission map shown by colour in Fig. 2. The normalization coefficient, X, shown on the map, is derived by using $X = 1\ {\rm sr}/(\pi R^2_{\rm outer} - \pi R^2_{\rm inner})$. Note that the template, *doughnut*, is homogeneous and, therefore, the possible variations of the gas column density over the H I gas structure are not taken into account.

The second spatial template is associated with the 'disc' inside the foreground emission doughnut-shaped structure in Fig. 2. This template, dubbed *disc*, corresponds to the inner region with a size of 1° of the Virgo cluster and is shown on the upper-right panel in Fig. 3. The values, X, on the map were derived via $X = 1\ {\rm sr}/(\pi R^2_{\rm inner})$. Note that the surface area of the *disc* template is ≈3.8 times smaller than that of the *doughnut* template. The number of *Fermi*-LAT photon events (as well as the incoming photon flux) associated with a spatial template, is expected to be proportional to the surface area of a template. Therefore, the DM annihilation signal from the *doughnut* template is expected to be stronger than that from the *disc* template. However, the γ-ray signal from DM annihilation is proportional to the integral along the line of sight of the squared mass density of DM, $J = \int \rho^2_{\rm DM} {\rm d}l$ and depends on the spatial DM distribution (thus, a cusped DM profile increases the DM annihilation signal from the inner part of the Virgo cluster).

The third and fourth spatial templates (dubbed *petals1* and *petals2* owing to their spatial shapes) are each composed of three distinct parts of equal surface areas. The centres of the three parts belonging to each of these spatial templates are located at the apices of an equilateral triangle. The third and fourth templates are shown on the lower-left and lower-right panels, respectively, in Fig. 3. The values, X, on the map were derived by using the rule, $X = 1\ {\rm sr}/(\pi R^2_{\rm outer}/2 - \pi R^2_{\rm inner}/2)$. The sum of the third and fourth templates (with equal weighting factors) is identical to the first template, *doughnut*, multiplied by a factor of 2. The *petals1* template covers the three prominent structures on the 1–3 GeV residual count map, while the *petals2* template does not spatially overlap with these structures. The DM distribution in the haloes of relaxed clusters is expected to be roughly spherically symmetrical and, therefore, the *petals1* and *petals2* templates should be useful to test the possible deviation from the continuous spherical symmetry of the DM distribution. Note that a large part of the mass of the Virgo cluster is centred on the galaxy M87, with smaller concentrations around M86 (at RA ≈ $186\overset{\circ}{.}55$, Dec. ≈ $12\overset{\circ}{.}95$) and M49 (at RA ≈ $187\overset{\circ}{.}44$, Dec. ≈ $8\overset{\circ}{.}00$), see, e.g. Böhringer et al. (1994). The mass concentration around M86 is part of a small group of galaxies that is merging with the main galaxy cluster. Thus, if the DM distribution is the

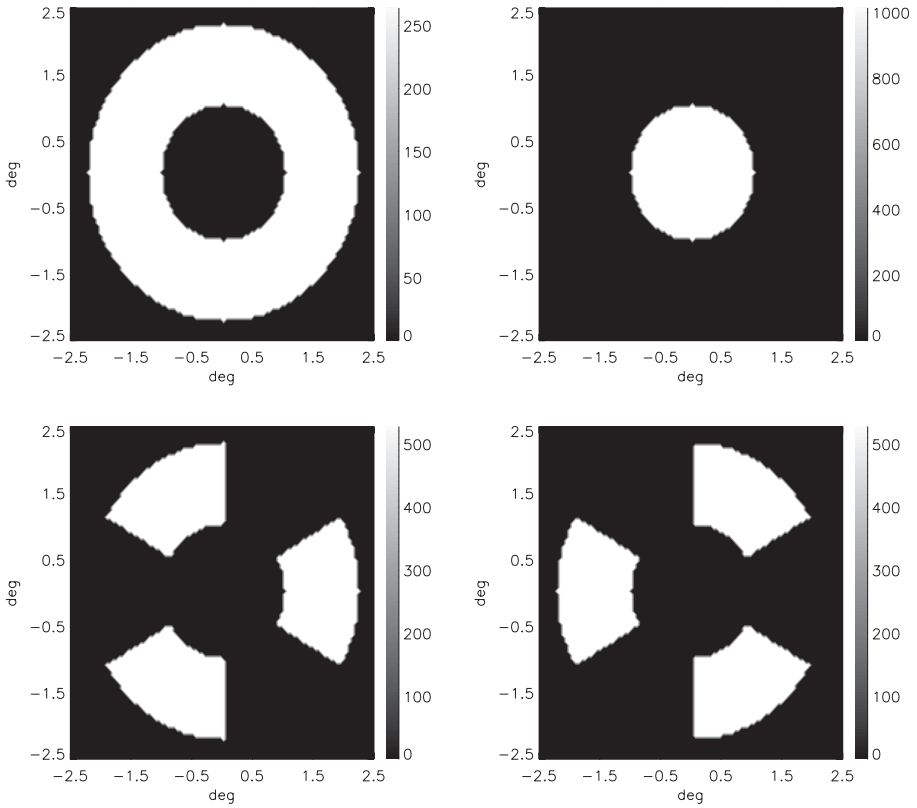

Figure 3. Templates used for the comparison of different models of the origin of the excess between 1 and 3 GeV from Virgo.

same as described by Böhringer et al. (1994), we expect that the model including the two spatial templates, *disc,* and *petals2*, should be the more statistically significant than that includes the spatial template *petals1*.

5.2 Morphological analysis

Morphological analysis is a problem-structuring technique of combining parameters into new combinations for later review. Below, we apply the morphological analysis to study the *Fermi*-LAT observations of the Virgo cluster in order to show that the residuals in the energy band where the DM annihilation spectrum has a prominent spectral feature can be successfully used for the search for extended γ-ray sources associated with DM annihilation.

We assume the presence of the possible additional components with different spatial distributions, which have not been included in the likelihood analysis in the previous section, and perform a likelihood analysis for the various models. The results of likelihood analyses are shown in Table 2. Model M0 is identical to that considered in the previous section, and includes the 2FGL point sources, galactic foreground, and isotropic background. Model M1 is nested with model M0 and includes the additional *doughnut* template with the photon spectrum given by equation (1), mimicking the possible DM annihilation spectrum. Models M2, M3, and M4 are also nested with model M0, and include the additional spatial templates *disc*, *petals1*, and *petals2*, respectively. Also for these templates the spectral distributions is described by equation (1). Each of the models M1, M2, M3, and M4, include one additional free parameter, the normalization of the spectrum of an additional component, compared with model M0.

Models M5 and M6 are more complex and include two additional templates; *petals1* + *petals2*, and *petals2* + *disc*, respectively. The spectral shapes of each of these components are given by equation (1) and their normalizations are independent free parameters in likelihood analyses. Model M5 is nested with models M0, M1, M3, and M4 whereas model M6 is nested with models M0, M2, and M4. The calculated log-likelihood values for the described models are shown in the fourth column of Table 2. The difference, multiplied by 2, between the log-likelihood function maximized by adjusting all the parameters of the model, with ($\log L_{\rm max,1}$) and without ($\log L_{\rm max,0}$, M0 in this case) the additional component, are shown in the fifth column of Table 2.

The model with an additional component (with free normalization) will always fit at least as well (have a greater log-likelihood) as the model without an additional component. To test whether the fit improved significantly, and should thus be preferred is determined by deriving the probability of the difference in the log-likelihoods. Where the null hypothesis represents a special case of the alternative hypothesis (i.e. the case of nested models), the probability distribution of the test statistics is approximately a chi-squared distribution with degrees of freedom equal to $df_2 - df_1$, where df_1 and df_2 represent the number of free parameters of the two candidate models. If we take model M0 as a null model, then using the fifth column of Table 2, we find that models M1, M3, and M5 significantly better describe the observational data than model M0 does. Comparing model M1 with M0, we find that the significance of the presence of the DM structure is 3.4σ. Comparing models M3 and M5 with M0, we find that the addition of the *petals1* template strongly improves the fit with a significance of 4.3σ for M3 model and 4.0σ for M5 model. As for models M2 and M4, our analysis demonstrates that the inclusion of either *disc* or *petals2* templates do not significantly improve the fit. Therefore, the observational data support the presence of the spatial structure associated with the template, *petals1*, and has no evidence for the presence of other additional spatial structures with the DM spectrum given by equation (1).

Models M1 and M5 are nested and their comparison with the observational data permits us to check if model M5 provides a significantly better fit than model M1. Since the template for model M5 is produced by using the high 1–3 GeV residuals, this template is not continuously symmetric with respect to the axis passed through the centre of the count map (i.e. the position of M87) along the line of sight (although this template has a discrete rotational symmetry of the sixth order, i.e. rotation by an angle of $360^\circ/6 = 60^\circ$ does not change the template), while the template for model M1 is continuously symmetric about this central axis. The comparison of these models is a test of the assumption about the continuously symmetry that has been made by Han et al. (2012a). The possible improvement is calculated by multiplying with two the difference between the log-likelihood of the models, M1 and M5 (the fourth column in Table 2). Therefore, the significance of the improvement of the fit by taking into account the two templates *petals1* and *petals2*, instead of the *doughnut* template is 2.7σ. At 2.7σ there is only 1 chance in nearly 150 that a random fluctuation would yield the result. Note that two sources from a new γ-ray population of seven point sources, proposed by Macías-Ramírez et al. (2012), and nearest to the centre of the Virgo cluster are covered by the *petals1* template. The coordinates of these two point sources are (RA, Dec.) = ($188\overset{\circ}{.}18$, $13\overset{\circ}{.}56$) and ($185\overset{\circ}{.}48$, $12\overset{\circ}{.}04$). This shows correspondence between the derived high significance of the spatial structure associated with the *petals1* template and the tentative point sources beyond the 2FGL catalogue. Although the *disc* template covers the central part of the Virgo cluster and that the *petals2* template covers the mass concentration around M87, the inclusion of these templates in the analysis (model M6) does not significantly improve the fit compared with that of the original model M0, see the fifth column of Table 2.

Thus, we have demonstrated that the residuals at 1–3 GeV allows us to create a template, *petals1*, which significantly improves the fit. Using a prominent feature of WIMP annihilation spectra and creating the spatial templates (covering the highest residuals in the energy band corresponding to the WIMP annihilation spectral feature), we have shown that the presented morphological analysis is a powerful approach for studying extended γ-ray sources and their possible association with signals from WIMP annihilation.

Table 2. The results of likelihood analyses. The difference in degrees of freedom Δ d.o.f., is compared to the M0 model.

Model	Template	Δ d.o.f.	$-\log(L)$	$2\log(L_{\rm max,1}/L_{\rm max,0})$
M0	–	–	312 042.20	–
M1	*doughnut*	1	312 036.37	11.66
M2	*disc*	1	312 040.88	2.64
M3	*petals1*	1	312 032.61	19.18
M4	*petals2*	1	312 041.35	1.7
M5	*petals1*+*petals2*	2	312 032.61	19.18
M6	*petals2*+*disc*	2	312 040.55	3.3

6 LIKELIHOOD ANALYSIS USING 5 YR OF DATA

The result of the analysis presented above shows that the additional extended γ-ray source in the region of the ISM doughnut-shaped

Table 3. The results of likelihood analyses of the 5 yr data.

Model	Template	Δ d.o.f.	$2\log(L_{\max,1}/L_{\max,0})$ 3.8 yr	5 yr
M0	–	–	–	–
M1	*doughnut*	1	14.12	20.06
M2	*disc*	1	4.29	4.37
M3	*petals1*	1	23.17	33.36
M4	*petals2*	1	2.11	2.83
M5	*petals1*+*petals2*	2	23.17	33.36
M6	*petals2*+*disc*	2	4.93	5.45

gas structure, that is located in the direction of the Virgo cluster, is statistically significant at 3.4σ level. This emission can be attributed to DM annihilation in the halo of the Virgo cluster or to non-2FGL point sources near the Virgo cluster (see Han et al. 2012b; Macías-Ramírez et al. 2012). It can also be caused by imperfections of the Galactic foreground model describing the ISM doughnut-shaped structure towards the Virgo cluster. To check these possibilities, we compared the two models M1 and M5 in Section 5.2 and found that the additional extended γ-ray source is spatially inhomogeneous, under the assumption that the Galactic foreground model is perfectly modelled. If these results hold, then we expect that:

(1) the significance of the doughnut template, *doughnut*, should increase with observation time, and
(2) the relative likelihood of model M5 (based on the template *petals1*+*petals2*) with respect to model M1 (based on the template *doughnut*) should increase with time.

The likelihood analyses was repeated using the data collected from 2008 August 4 to 2013 July 25. The results of the likelihood analyses are shown in Table 3. The models and parameters shown in this table are the same as those shown in Table 2 and are described in the second paragraph of Section 5.2.

Using the fourth column of Table 3, we found that the statistical significance of the *doughnut* template is 4.5σ. We also found that the statistical significance of the *petals1* template is 5.8σ and the statistical significance of the *petals2* template is only 1.7σ. The significance of the improvement of the fit by taking into account the two templates *petals1* or *petals2* instead of the *doughnut* template is 3.7σ. At 3.7σ there is only one chance in nearly 3800 that a random fluctuation would yield the result. This provides strong evidence that the potential extended source, located in the region of the ISM doughnut-shaped structure, is spatially inhomogeneous. Therefore, the results reported in the previous sections hold when the first 5 yr of the *Fermi*-LAT data are analysed.

7 CONCLUSION

In this paper, we develop a morphological analysis method and demonstrate its use for the search for the possible extended γ-ray sources associated with DM annihilation. This approach is based on the analysis of morphology of residual count maps using spatial templates and by taking into account a prominent spectral feature of WIMP annihilation. We chose the photon spectrum produced via annihilation of WIMPs with a mass of $M \simeq 28$ GeV as an example, since the possible signals from annihilation of WIMPs with such masses have recently been discussed by Hooper & Linden (2011) and Han et al. (2012a) in their analyses of the *Fermi*-LAT observations of the Galactic Centre and Virgo region, respectively.

The PSF of the *Fermi*-LAT instrument has a 68 per cent containment radius of about 6° at 100 MeV and $0.^\circ2$ at 100 GeV. The PSF is about 1° at 1 GeV and *Fermi*-LAT therefore allows us to spatially resolve nearby clusters of galaxies. The detection of the nearest galaxy clusters, such as Virgo and Coma, is one of goals of the *Fermi* mission. A γ-ray signal from galaxy clusters can be dominated by photons produced via DM annihilation. Other extended γ-ray sources where WIMP annihilation photons can potentially contribute to the emission are the Galactic Centre and the DM halo of the Andromeda galaxy.

DM particles annihilation in astrophysical sources allows us to perform indirect searches for DM. We consider the process $\chi\chi \rightarrow b\bar{b}$, the annihilation of pairs of DM particles to pairs of b quarks. Spectra of photons produced in hadronic processes have a peak at an energy of $E_{\rm peak} \approx m_\chi/25$ (e.g. see Baltz et al. 2007). If a DM particle mass has a mass of 25 GeV, then the peak in the photon spectrum is expected at $\simeq$1 GeV. Therefore, the residual count map at the peak energy, produced by subtracting the model (without the inclusion of a WIMP annihilation source) from the observational data, could give valuable information about the spatial morphology of a possible WIMP annihilation source. Note that point like γ-ray sources with hard spectra at low energies and with a spectral exponential cut-off at high energy equally well describe pulsar and WIMP annihilation in γ-rays. Therefore, the extended γ-ray sources associated with a high concentration of DM provide us with a unique possibility to search for WIMP annihilation γ-ray signals.

We applied a morphological analysis to the study of the Virgo cluster initially assuming the presence of 2FGL sources, Galactic diffuse foreground, and extragalactic diffuse background. We derived the 1–3 GeV residual count map and found that the high residuals at 1–3 GeV are confined in three spatial regions, and that the morphology of residuals is clumpy rather than continuously spherically symmetric. We performed a likelihood analysis using 3.8 yr of *Fermi*-LAT observations. Different spatial templates, dubbed *doughnut*, *disc*, *petals1*, and *petals2*, were obtained by taking into account the morphology of the high 1–3 GeV residuals. Our analysis demonstrates that the presence of the template, *petals1*, covering the high 1–3 GeV residuals and having the photon spectrum provided by WIMP annihilation, strongly improves the fit. The significance of the extended emission using the *petals1* template is 4.3σ. The *doughnut* template is continuously spherically symmetric, spatially covers the high 1–3 GeV residuals, and its surface is two times larger than the surface of a *petals1* template. The significance of the improvement of the fit by taking into account the two templates, *petals1* or *petals2* (with equal surface areas) instead of the continuously symmetric template, *doughnut*, is 2.7σ. This shows that the γ-ray signal which could be associated with WIMP annihilation is not continuously symmetric in the inner part of the Virgo cluster. This result can be explained by the presence of new point sources not included in the 2FGL catalogue or by the uncertainties in modelling of the Galactic foreground emission in the direction of the Virgo cluster. Therefore, the morphology of residuals at the energy peak of the photon spectra corresponding to those of WIMP annihilation provides an interesting diagnostic of a potential DM distribution. In Section 6, we demonstrated that the conclusion on inhomogeneity of the possible extended source towards the Virgo cluster holds when the first 5 yr of *Fermi*-LAT observations are analysed. Studying of the morphology of residual count maps at such energies can be used for a search for extended γ-ray signals from WIMP annihilation.

REFERENCES

Abdo A. A. et al., 2009, ApJ, 707, 55
Ackermann M. et al., 2010a, J. Cosmol. Astropart. Phys., 5, 25
Ackermann M. et al., 2010b, ApJ, 717, L71
Ackermann M. et al., 2012a, ApJ, 747, 121
Ackermann M. et al., 2012b, ApJ, 750, 3
Ackermann M. et al., 2013, preprint (arXiv:1308.5654)
Ackermann M. et al., 2014, Phys. Rev. D., 89, 042001
Ando S., Nagai D., 2012, J. Cosmol. Astropart. Phys., 7, 17
Atwood W. B. et al., 2009, ApJ, 697, 1071
Auld R. et al., 2013, MNRAS, 428, 1880
Baltz E. A., Taylor J. E., Wai L. L., 2007, ApJ, 659, L125
Bertone G., Hooper D., Silk J., 2005, Phys. Rep., 405, 279
Böhringer H., Briel U. G., Schwarz R. A., Voges W., Hartner G., Trümper J., 1994, Nature, 368, 828
Burnham K. P., Anderson D. R., 2002, Model Selection and Multimodel Inference: A Practical Information-Theoretic Approach. Springer-Verlag, Berlin
Davies J. I. et al., 2010, A&A, 518, L48
Gao L., Frenk C. S., Jenkins A., Springel V., White S. D. M., 2012, MNRAS, 419, 1721
Han J., Frenk C. S., Eke V. R., Gao L., White S. D. M., 2012a, preprint (arXiv:1201.1003)
Han J., Frenk C. S., Eke V. R., Gao L., White S. D. M., Boyarsky A., Malyshev D., Ruchayskiy O., 2012b, MNRAS, 427, 1651
Hooper D., Linden T., 2011, Phys. Rev. D., 84, 123005
Huang X., Vertongen G., Weniger C., 2012, J. Cosmol. Astropart. Phys., 1, 42
Kalberla P. M. W., Burton W. B., Hartmann D., Arnal E. M., Bajaja E., Morras R., Pöppel W. G. L., 2005, A&A, 440, 775
Lande J. et al., 2012, ApJ, 756, 5
Ludlow A. D., Navarro J. F., Angulo R. E., Boylan-Kolchin M., Springel V., Frenk C., White S. D. M., 2013, preprint (arXiv:1312.0945)
Macías-Ramírez O., Gordon C., Brown A. M., Adams J., 2012, Phys. Rev. D., 86, 076004
Mattox J. R. et al., 1996, ApJ, 461, 396
Miniati F., 2003, MNRAS, 342, 1009
Nolan P. L. et al., 2012, ApJS, 199, 31
Pinzke A., Pfrommer C., Bergström L., 2011, Phys. Rev. D., 84, 123509
Porter T. A., Johnson R. P., Graham P. W., 2011, ARA&A, 49, 155
Prokhorov D. A., Churazov E. M., 2013, preprint (arXiv:1309.0197)
Sanchez-Conde M. A., Prada F., 2013, preprint (arXiv:1312.1729)
Sarazin C. L., 1986, Rev. Mod. Phys., 58, 1
Trimble V., 1987, ARA&A, 25, 425

This paper has been typeset from a TEX/LATEX file prepared by the author.